



Published in final edited form as:

Vet Pathol. 2012 July ; 49(4): 636–641. doi:10.1177/0300985811406890.

Pleural Endometriosis in an Aged Rhesus Macaque (*Macaca Mulatta*): A Histopathologic and Immunohistochemical Study

Basel T. Assaf and Andrew D. Miller

New England Primate Research Center, Harvard Medical School, Division of Comparative Pathology, Southborough, MA 01772

Abstract

Endometriosis is defined as the presence of endometrial tissue outside the uterine cavity and is one of the most common reproductive abnormalities encountered in women as well as Old World primates. The majority of endometriosis cases in Old World primates occur within the abdominal cavity, with spread to extraabdominal sites considered to be a rare event. A 19-year-old multiparous female rhesus macaque (*Macaca mulatta*) presented to necropsy for difficulty breathing and weight loss. Grossly, the animal had marked abdominal endometriosis and severe hemoabdomen and hemothorax, the latter of which was accompanied by marked pleural fibrosis. Histologic examination confirmed the abdominal endometriosis and also revealed numerous uterine glands and stroma embedded within the pleural fibrosis. Rafts of endometrial tissue were present within pulmonary lymphatics and the tracheobronchial lymph nodes.

Immunohistochemically, all ectopic endometrial tissue had varying degrees of positive immunoreactivity to cytokeratin, vimentin, progesterone and estrogen receptors, and calretinin but was negative for desmin and carcinoembryonic antigen. Pleural endometriosis is an extremely rare manifestation of endometriosis in nonhuman primates. This case report emphasizes lymphatic spread as a likely mechanism for extrauterine endometriosis.

Keywords

Macaca mulatta; endometriosis; thoracic; fibrosis; calretinin

Introduction

Endometriosis is characterized by extrauterine growth and proliferation of endometrial glandular and stromal cells in menstruating primates.^{12,21} The lesion is grossly recognized by the presence of multiple red–brown “chocolate” cysts in the abdominal cavity that progress to white fibrotic scars with adhesions to adjacent organs, depending on the age and severity of the lesion and the stage of menstrual cycle.²³ Histologically, the cysts are filled with blood that is surrounded by endometrial glands, endometrial stroma, hemosiderin-laden macrophages, and fibrosis.⁴ All structures in the pelvic and extrapelvic abdominal cavity can be involved, and in rare cases, there can be extension to the thoracic cavity.¹² Three theories have been postulated to explain the development of endometriosis.^{12,21,25} The most widely accepted theory is the implantation, or Sampson’s, theory, which proposes that retrograde menstruation leads to endometrial tissue that passes through the lumen of the Fallopian tubes and into the peritoneal cavity.^{17,25} The endometrial tissue then implants along the serosa and proliferates, often invading and incarcerating adjacent organs. The second theory

proposes that endometriosis develops from metaplasia of cells lining serosal surfaces, including the abdominal and thoracic structures. This theory has been used to explain the development of endometriosis in locations where retrograde menstrual flow is impossible. Lastly, the induction theory combines the implantation and metaplasia theories and proposes that retrograde menstruation produces substances that induce metaplasia of peritoneal serosa. Despite the multiple theories, no single theory is capable of explaining all cases of endometriosis, and the disease likely has multiple causes. Various hypotheses have been proposed to explain intrathoracic dissemination of ectopic uterine tissue and include transabdominal–transdiaphragmatic endometrial tissue explantation, lymphatic and/or hematogenous spread, and coelomic metaplasia.² Despite its rarity in women, intrathoracic endometriosis is the only cause of catamenial (recurring monthly with menstruation) pneumothorax, hemothorax, and hemoptysis in women, and several human cases report secondary fibrosis.^{2,11}

Animal models provide an extremely valuable tool to facilitate research on the etiology and pathophysiology of endometriosis.²³ Besides Old World primate species, many nonprimate species have been used to induce endometriosis following autologous transplantation of uterine tissue into the peritoneum of mice, rabbits, rats, and hamsters.^{19,20,22,24} Despite the low cost, easy handling, and ability to genetically manipulate nonprimate animal models, the wide evolutionary gap between primates and these other species, the lack of a menstrual cycle, and the lack of spontaneous endometriosis in nonprimate species make inferences quite difficult from these animal models.^{5,23} In Old World primates, spontaneous and induced forms of endometriosis have been widely studied, primarily in rhesus macaques and baboons, and spontaneous endometriosis is commonly found in multiparous animals at necropsy.¹³ The first case of spontaneous endometriosis in a rhesus macaque was reported by Fraser in 1929, followed by numerous reports of spontaneously occurring and experimentally induced endometriosis.⁹ Spontaneous endometriosis has been reported in captive colonies of female rhesus macaques with incidences as high as 25%.⁷ Spontaneous endometriosis in the nonhuman primate mimics its human counterpart in both morphology and dissemination.⁶

Despite extensive research on endometriosis in rhesus macaques, only a single case of intrathoracic endometriosis was briefly reported in 1971.¹⁴ Herein, we describe the morphologic and immunohistochemical characterization of intrathoracic endometriosis and provide a discussion on the origin and mode of dissemination of intrathoracic endometriosis.

Materials and Methods

The animal—a normally cycling multiparous female rhesus macaque aged 19 years was born at the New Iberia Research Center and raised and housed at the New England Primate Research Center in a biosafety level 2 facility in accordance with the National Research Council's Guide for the Care and Use of Animals and the standards of the Harvard Medical School Standing Committee on Animals and the Association for the Assessment and Accreditation of Laboratory Animal Care. The animal was screened annually for simian retrovirus D, simian T-lymphotropic virus, simian immunodeficiency virus, and *Macacine herpesvirus 1* (B virus) via serology, and negative tuberculosis status was confirmed via quarterly intradermal testing.

Necropsy was conducted within 2 hours of euthanasia, and representative sections of all major organs were collected, fixed in 10% neutral buffered formalin, embedded in paraffin, sectioned at 5 mm, and stained using hematoxylin and eosin. Additional sections were stained with periodic acid–Schiff. Sections for immunohistochemistry were prepared according to a routine protocol. Briefly, formalin-fixed, paraffin-embedded sections were

deparaffinized, rehydrated, and subsequently blocked with hydrogen peroxide. Pretreatment for estrogen receptor, progesterone receptor, or calretinin involved microwaving for 20 minutes in 0.01M citrate buffer, followed by 20 minutes of cooling. Pretreatment for vimentin, cytokeratin, or carcinoembryonic antigen (CEA) was proteinase K at room temperature for 5 minutes; the desmin antibody did not require a pretreatment. All steps were followed by a tris-buffered saline wash. Prior to application of primary antibodies, all slides were treated with a protein block (Dako, Carpinteria, CA) for 10 minutes. Sections were incubated with anti-human progesterone receptor (Dako; monoclonal, 1:50, overnight in refrigerator), anti-human estrogen receptor (Dako; monoclonal, 1:100, overnight in refrigerator), anti-human vimentin (Dako; monoclonal, 1:162, overnight in refrigerator), anti-rabbit calretinin (Zymed, San Francisco, CA; polyclonal, 1:50, 60 minutes at room temperature), anti-human cytokeratin AE1/AE3 (Dako; monoclonal, 1:140, overnight in refrigerator), anti-human CEA (Dako; polyclonal, 1:400, 30 minutes at room temperature), and anti-human desmin (Dako; polyclonal, 1:50, overnight in refrigerator). Slides were then incubated with secondary antibody biotinylated goat anti-rabbit (Vector Laboratories, Burlingame, CA; 1:200, 30 minutes at room temperature) for calretinin and CEA and with biotinylated horse anti-mouse (Vector Laboratories; 1:200, 30 minutes at room temperature) for progesterone receptor, estrogen receptor, vimentin, cytokeratin AE1/AE3, and desmin. This was followed by a 30-minute incubation at room temperature with Vectastain ABC Elite (Vector Laboratories; progesterone receptor, estrogen receptor, cytokeratin AE1/AE3, calretinin) or Vectastain ABC Standard (Vector Laboratories; vimentin, CEA, desmin). All slides were developed with DAB chromogen (Dako) and counterstained with Mayer's hematoxylin. In all cases, step sections were incubated with isotype-specific irrelevant antibodies for negative controls. Positive controls for all antibodies consisted of rhesus macaque uterus.

Results

Clinical and Gross Features

The animal, with a history of 7 pregnancies and 2 stillbirths, was presented to necropsy for chronic weight loss, generalized poor health, and dyspnea on the day of euthanasia. Complete blood count and clinical chemistry revealed a nonregenerative, normocytic, normochromic anemia, with mild lymphopenia and neutropenia, mild azotemia, and mild hypoalbuminemia. Grossly, the animal had numerous red, raised masses (0.5 to 4 cm diameter) scattered throughout the abdominal cavity. This was accompanied by numerous adhesions between abdominal organs and less than 10 ml of red-tinged peritoneal fluid. Within the thoracic cavity, the pleura was markedly thickened and opaque with multiple adhesions between the lungs, costal pleura, and diaphragm. Lung lobes were collapsed and consolidated with multifocally pale to light brown discolorations. The thoracic cavity contained roughly 20 ml of red-tinged fluid.

Histopathologic Features

Histologically scattered throughout the pleural surface were multiple, unencapsulated, variably sized nodules composed of densely cellular spindle-shaped stromal cells in which were frequently embedded uterine-like glands (Fig. 1). The glands were lined by simple to pseudostratified columnar, occasionally ciliated epithelial cells with a moderate amount of pale eosinophilic cytoplasm and prominent basilar oval-shaped nuclei. These nodules were often admixed with scattered lymphocytes, nondegenerate neutrophils, hemorrhage, and hemosiderin-laden macrophages. The glands infrequently contained a mucinous secretion (Fig. 2). The stromal cells had indistinct cell borders, scant eosinophilic cytoplasm, and an oval to elongate nucleus. The pleura was diffusely thickened by varying degrees of fibrosis and edema that was admixed with numerous histiocytes, hemosiderin-laden macrophages,

lymphocytes, neutrophils, and, rarely, Langhans giant cells (Fig. 3, inset). The lumina of blood vessels within the pleura were variably occluded by partially organized fibrin thrombi. Groups of cuboidal to low columnar epithelial cells identical to those in the ectopic endometrial glands were present within lymphatic vessels (Fig. 4). The subpleural pulmonary parenchyma was multifocally expanded by areas of marked fibrosis and edema. These areas were admixed with variable numbers of histiocytes, hemosiderin-laden macrophages, and lymphocytes.

Similar endometriotic lesions admixed with hemorrhage and hemosiderin-laden macrophages were present on the thoracic and abdominal side of the diaphragm. Ectopic endometrial glands were present within the subcapsular sinuses of tracheobronchial lymph node (Figs. 5, 6). Lastly, endometriotic masses were present and scattered throughout the abdominal cavity, including but not limited to the uterine serosa, the serosa of the urinary bladder, and the serosa of the small intestine. Comorbid histologic findings included fibrosing pericarditis and uterine leiomyoma, as well as necrotizing pulmonary, coronary, renal, and pancreatic arteritis.

Immunohistochemical Features

Immunohistochemical results are shown in Table 1. The endometrial glands embedded within the pleura had strong and diffuse cytoplasmic immunoreactivity to pancytokeratin (Fig. 7). Normal endometrium had similar, strong intracytoplasmic, intraepithelial immunoreactivity (Fig. 8). Immunoreactivity for progesterone receptor in the pleural endometriosis was strongest in the stroma and less intense in the epithelial cells (Fig. 9). Progesterone receptor immunoreactivity in the normal endometrium had a similar distribution; however, the epithelial intensity was greater (Fig. 10). Immunoreactivity for estrogen receptor in the pleural endometriosis was nuclear and weak in both the stroma and the epithelium (Fig. 11). Estrogen receptor immunoreactivity in the normal endometrium had a similar distribution; however, the epithelial intensity was greater (Fig. 12). The ectopic endometrial glands and stroma displayed strong intracytoplasmic immunoreactivity for vimentin, which was strongest in the stroma and weakest in the epithelial cells (Fig. 13). Normal endometrium displayed little vimentin immunoreactivity in the epithelium and varied staining in the stroma (discounting vascular immunoreactivity) (Fig. 14). Ectopic uterine glandular tissue had no immunoreactivity for calretinin; however, there was variable immunoreactivity in the ectopic uterine stroma (Fig. 15). The normal uterus has a similar immunoreactivity for calretinin; however, the stroma was more intensely positive (Fig. 16). There was no immunoreactivity detected for desmin and CEA in either the ectopic uterine tissue or the normal uterus (data not shown).

Discussion

Endometriosis is a commonly reported disorder in adult female macaque species; however, the literature lacks a detailed histologic and immunohistochemical description of intrathoracic endometriosis despite numerous reports of a similar manifestation in human patients with endometriosis.⁷ In humans, episodes of catamenial shortness of breath and chest pain are frequently associated with cases of pleural endometriosis.^{2,8} A similar episodic nature to the dyspnea reported in this animal was not observed; however, the histologic lesions of pleural endometriosis and fibrosis were severe and would have likely led to persistent respiratory distress.

The origin and dissemination of endometriosis to intraabdominal and extra-abdominal cavities are debatable; however, there is an increased incidence in multiparous animals similar to the one presented herein. While implantation of regurgitated menstrual material is the most commonly accepted theory, direct implantation fails to explain dissemination of

endometriosis to tissue outside the abdominal cavity.^{12,21,25} The association of thoracic endometriosis with congenital or acquired diaphragmatic defects led to the proposed hypothesis of endometrial tissue invasion of thoracic cavity through a transabdominal–transdiaphragmatic dissemination.^{1–3} No such diaphragmatic defect was present in the current case, and the presence of endometrial tissue within pulmonary lymphatics and the tracheobronchial lymph node illustrates that lymphatic and hematogenous dissemination of endometrial tissue is an important mechanism of extrapelvic endometriosis.^{2,25} How endometrial stroma and glandular epithelium gain access to blood and lymph spaces is currently unknown.

The histomorphology and immunohistochemical immunoreactivity for pancytokeratin, vimentin, estrogen receptor, and progesterone receptor are consistent with ectopic endometrial tissue.^{10,15} The combination of uterine stromal cells surrounding small islands of glands is prototypical for endometriosis and excludes more common pleural neoplasms, such as mesothelioma and metastatic carcinomas or sarcomas. Negative CEA and desmin immunoreactivity further excludes adenocarcinomas and muscle neoplasms, respectively. Biphasic mesotheliomas are strongly positive for calretinin and negative for estrogen and progesterone receptors; the lack of strong calretinin immunoreactivity in this case makes the diagnosis of mesothelioma unlikely.^{16,18}

In conclusion, this report describes the first detailed morphologic and immunohistochemical characteristics of intrathoracic endometriosis in rhesus macaques. Ectopic pleural endometrial tissue resembled its counterpart in the normal uterus, and immunohistochemical staining was consistent within ectopic endometrial tissue. Although rare, intrathoracic endometriosis should be among the differential diagnosis for respiratory disease in macaque species, especially those associated with anemia. Based on intralymphatic plugs of endometriotic tissue, spread to the lungs in this case appears to have been via the lymphatic system.

Acknowledgments

The authors would like to thank Kristen Toohey for photographic assistance.

References

1. Alifano M, Roth T, Broet SC, Schussler O, Magdeleinat P, Regnard JF. Catamenial pneumothorax: a prospective study. *Chest*. 2003; 124:1004–1008. [PubMed: 12970030]
2. Alifano M, Trisolini R, Cancellieri A, Regnard JF. Thoracic endometriosis: current knowledge. *Ann Thorac Surg*. 2006; 81:761–769. [PubMed: 16427904]
3. Bagan P, Le Pimpec Barthes F, Assouad J, Souilamas R, Riquet M. Catamenial pneumothorax: retrospective study of surgical treatment. *Ann Thorac Surg*. 2003; 75:378–381. discussion 381. [PubMed: 12607643]
4. Clement PB. The pathology of endometriosis: a survey of the many faces of a common disease emphasizing diagnostic pitfalls and unusual and newly appreciated aspects. *Adv Anat Pathol*. 2007; 14:241–260. [PubMed: 17592255]
5. D'Hooghe TM, Kyama CM, Chai D, Fassbender A, Vodolazkaia A, Bokor A, Mwenda JM. Nonhuman primate models for translational research in endometriosis. *Reprod Sci*. 2009; 16:152–161. [PubMed: 19208783]
6. Dick EJ Jr, Hubbard GB, Martin LJ, Leland MM. Record review of baboons with histologically confirmed endometriosis in a large established colony. *J Med Primatol*. 2003; 32:39–47. [PubMed: 12733601]
7. Fanton JW, Golden JG. Radiation-induced endometriosis in *Macaca mulatta*. *Radiat Res*. 1991; 126:141–146. [PubMed: 1850850]

8. Flieder DB, Moran CA, Travis WD, Koss MN, Mark EJ. Pleuro-pulmonary endometriosis and pulmonary ectopic decidualis: a clinicopathologic and immunohistochemical study of 10 cases with emphasis on diagnostic pitfalls. *Hum Pathol.* 1998; 29:1495–1503. [PubMed: 9865838]
9. Fraser AD. Ectopic Endometrium in a Macacus Rhesus. *Journal of Obstetrics and Gynaecology of the British Empire.* 1929; 36:590–591.
10. Jones RK, Bulmer JN, Searle RF. Immunohistochemical characterization of proliferation, oestrogen receptor and progesterone receptor expression in endometriosis: comparison of eutopic and ectopic endometrium with normal cycling endometrium. *Hum Reprod.* 1995; 10:3272–3279. [PubMed: 8822457]
11. Joseph J, Sahn SA. Thoracic endometriosis syndrome: new observations from an analysis of 110 cases. *Am J Med.* 1996; 100:164–170. [PubMed: 8629650]
12. Lora Hedrick Ellenson, ECP. The female genital tract. In: Vinay Kumar, AKA.; Fausto, Nelson; Aster, Jon, editors. *Robbins and Cotran Pathologic Basis of Disease.* 8. Saunders Elsevier; Philadelphia: 2010. p. 1028-1029.
13. Mattison JA, Ottinger MA, Powell D, Longo DL, Ingram DK. Endometriosis: clinical monitoring and treatment procedures in Rhesus Monkeys. *J Med Primatol.* 2007; 36:391–398. [PubMed: 17976046]
14. McClure HM, Ridley JH, Graham CE. Disseminated endometriosis in a Rhesus monkey (*Macaca mulatta*). Histogenesis and possible relationship to irradiation exposure 1,2. *J Med Assoc Ga.* 1971; 60:11–13. [PubMed: 4992511]
15. Nisolle M, Casanas-Roux F, Donnez J. Coexpression of cytokeratin and vimentin in eutopic endometrium and endometriosis throughout the menstrual cycle: evaluation by a computerized method. *Fertil Steril.* 1995; 64:69–75. [PubMed: 7540565]
16. Ordenez NG. Value of estrogen and progesterone receptor immunostaining in distinguishing between peritoneal mesotheliomas and serous carcinomas. *Hum Pathol.* 2005; 36:1163–1167. [PubMed: 16260268]
17. Sampson J. Peritoneal endometriosis due to the menstrual dissemination of endometrial tissue into the peritoneal cavity. *Am J Obstet Gynecol.* 1927; 14:422–469.
18. Saydan N, Salicio V, Cappelli-Gotzos B, Gotzos V. Expression of calretinin in human mesothelioma cell lines and cell cycle analysis by flow cytometry. *Anticancer Res.* 2001; 21:181–188. [PubMed: 11299732]
19. Schenken RS, Asch RH. Surgical induction of endometriosis in the rabbit: effects on fertility and concentrations of peritoneal fluid prostaglandins. *Fertil Steril.* 1980; 34:581–587. [PubMed: 7450077]
20. Somigliana E, Vigano P, Rossi G, Carinelli S, Vignali M, Panina-Bordignon P. Endometrial ability to implant in ectopic sites can be prevented by interleukin-12 in a murine model of endometriosis. *Hum Reprod.* 1999; 14:2944–2950. [PubMed: 10601076]
21. Stanley, J.; Robboy, AH.; Russell, Peter. Endometriosis. In: George, L.; Mutter, M.; Prat, Jaime, editors. *Robboy's Pathology of the Female Reproductive Tract.* 2. Churchill Livingstone; 2009. p. 1104
22. Steinleitner A, Lambert H, Suarez M, Serpa N, Robin B, Cantor B. Periovarian calcium channel blockade enhances reproductive performance in an animal model for endometriosis-associated subfertility. *Am J Obstet Gynecol.* 1991; 164:949–952. [PubMed: 2014846]
23. Story L, Kennedy S. Animal studies in endometriosis: a review. *Ilar J.* 2004; 45:132–138. [PubMed: 15111732]
24. Vernon MW, Wilson EA. Studies on the surgical induction of endometriosis in the rat. *Fertil Steril.* 1985; 44:684–694. [PubMed: 4054348]
25. Witz CA. Pathogenesis of endometriosis. *Gynecol Obstet Invest.* 2002; 53 (Suppl 1):52–62. [PubMed: 11834869]

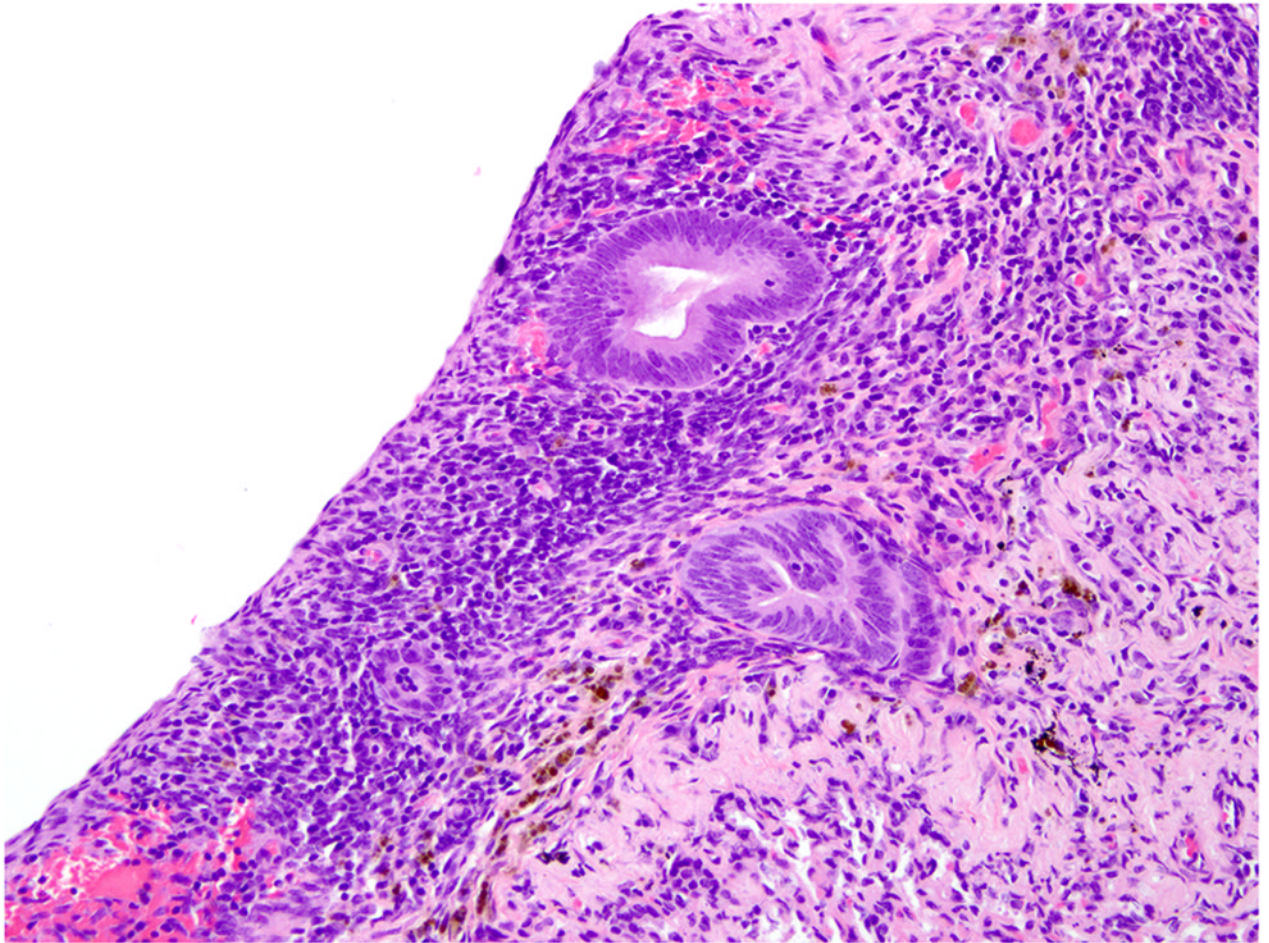


Figure 1. Lung pleura; rhesus macaque. Multifocally, endometrial glands and stromal cells are embedded within the pleura. HE.

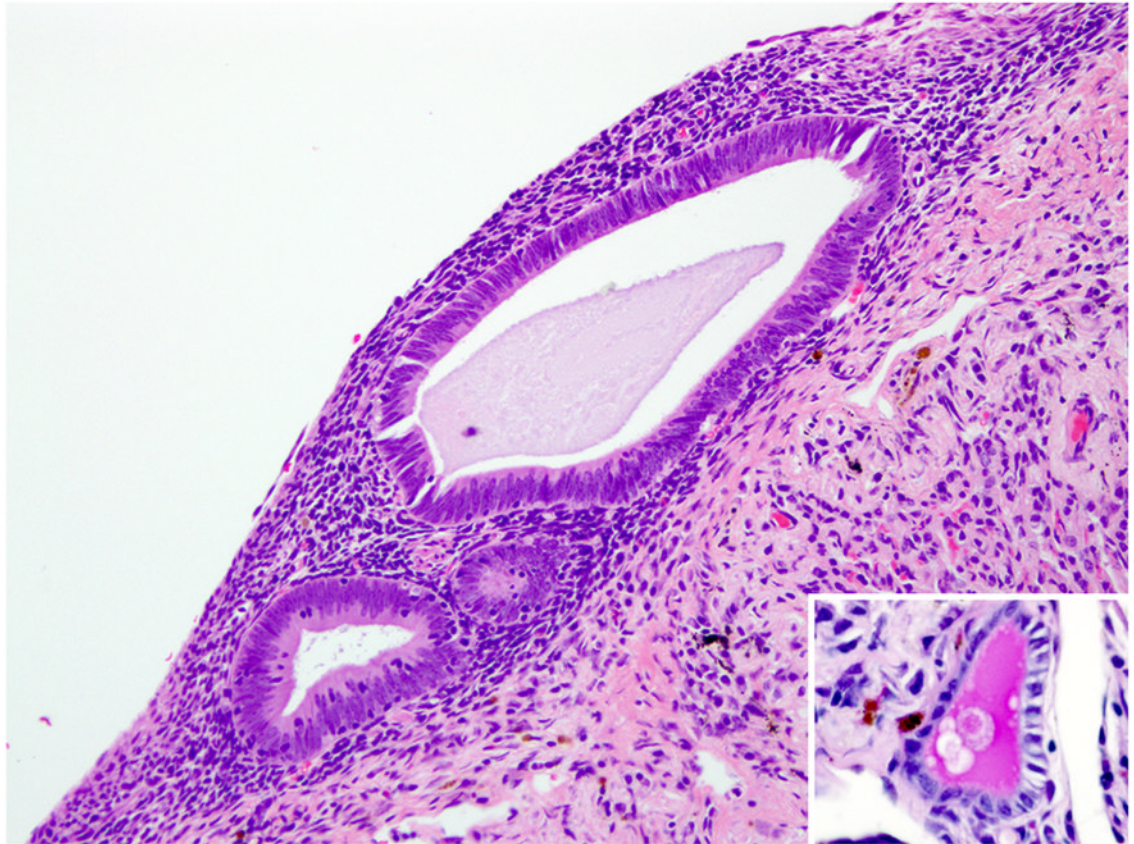


Figure 2. Lung pleura; rhesus macaque. Glands are lined by pseudostratified columnar epithelial cells that infrequently contain a mucinous secretion (inset; periodic acid Schiff). HE.

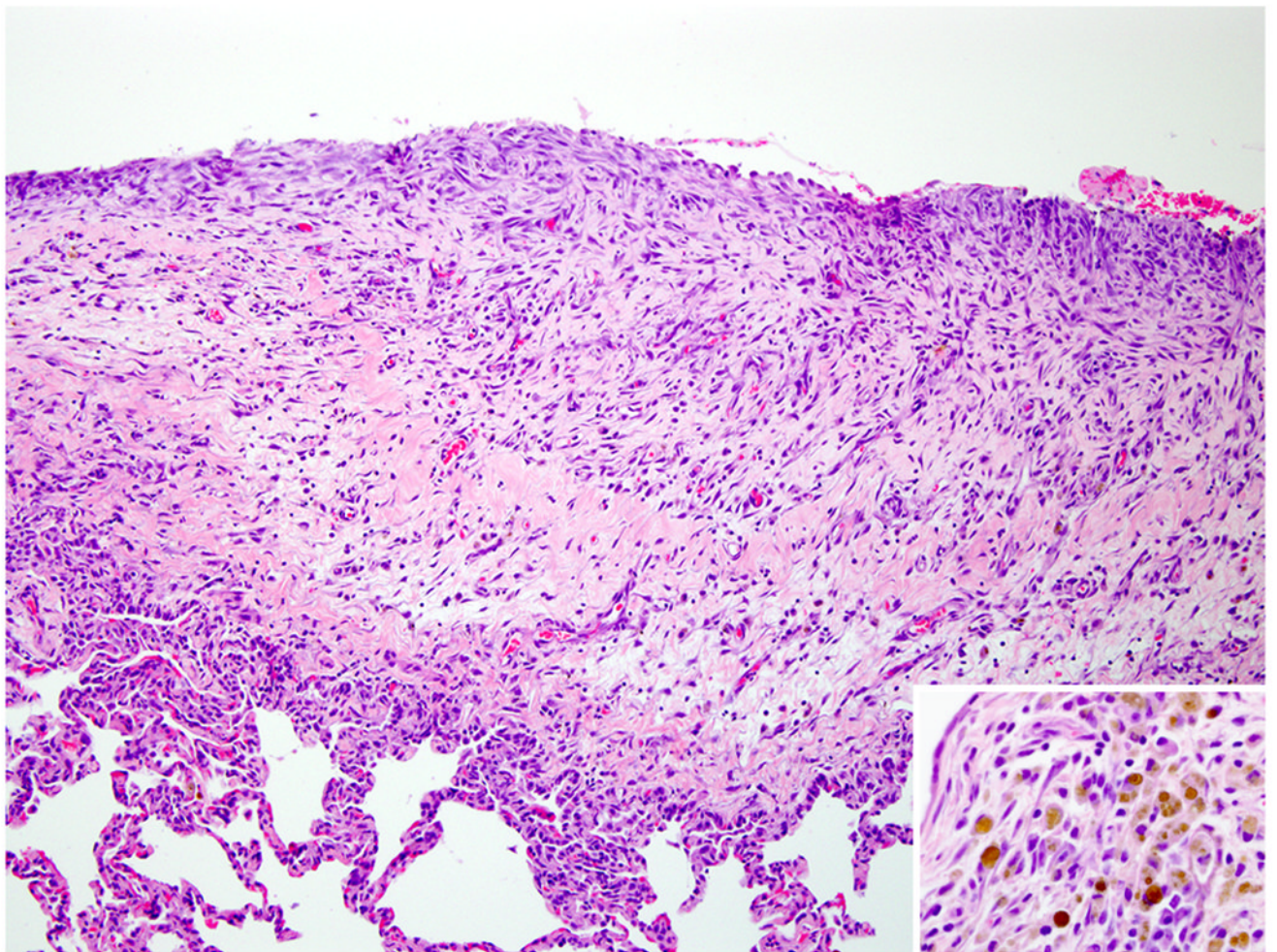


Figure 3. Lung pleura; rhesus macaque. The pleura is diffusely thickened by marked fibrosis and edema admixed with numerous hemosiderin-laden macrophages and a mixed inflammatory reaction (inset). HE.

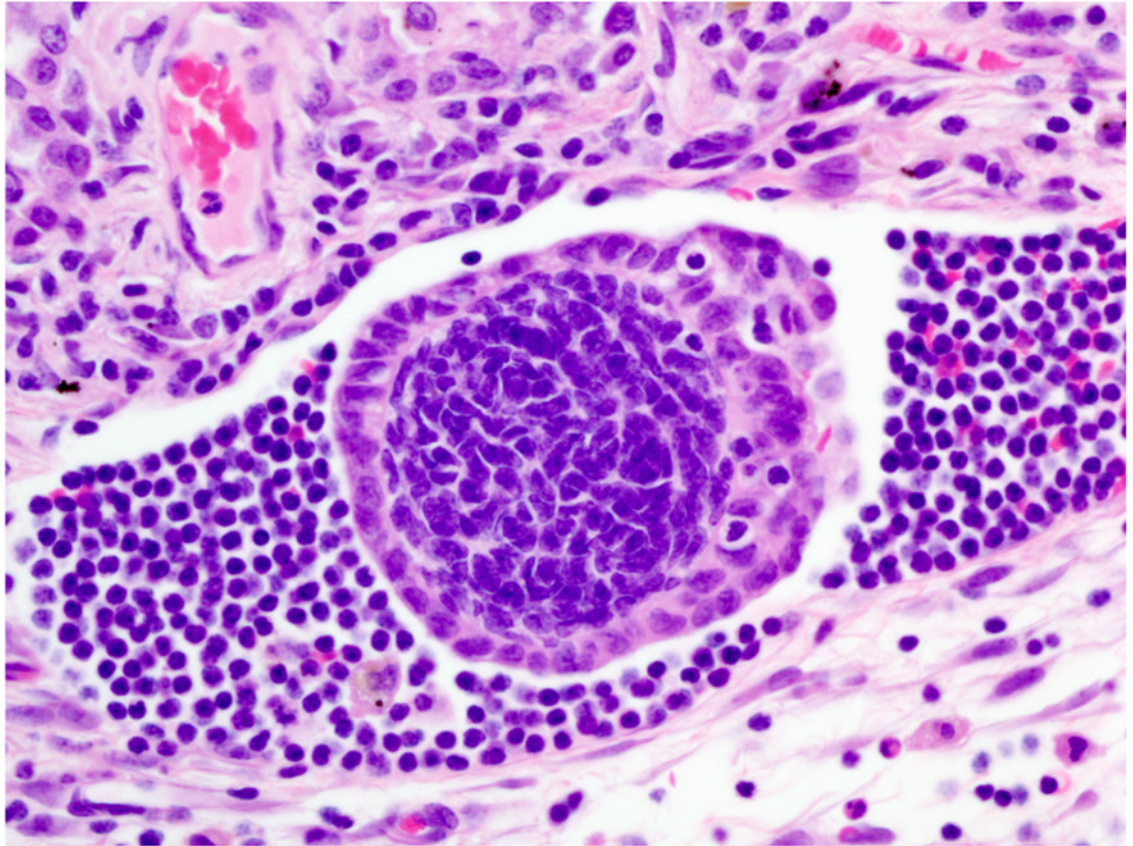


Figure 4. Lung; rhesus macaque. Aggregates of endometrial glands are present within lymphatic vessels. HE.

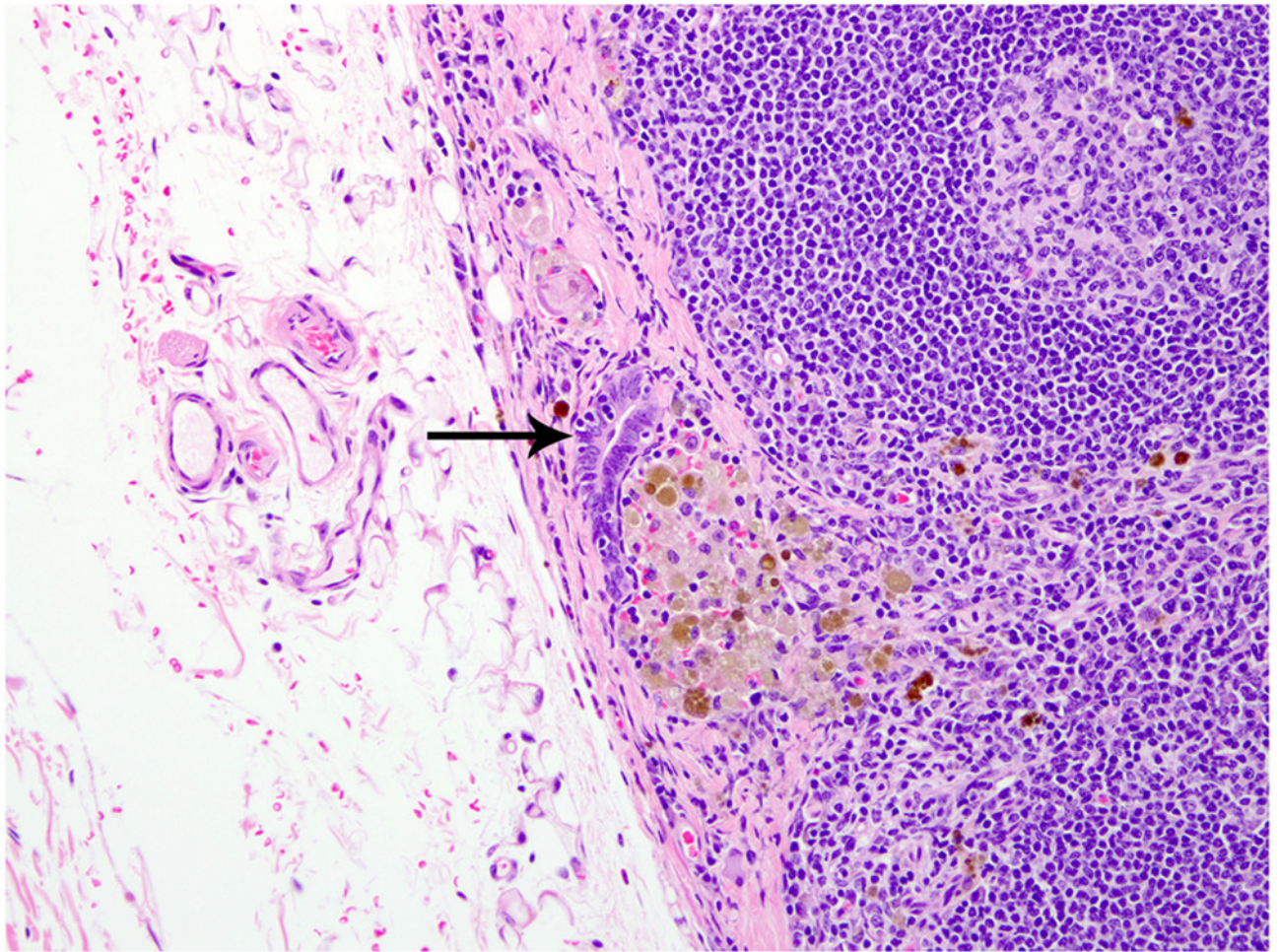


Figure 5. Tracheobronchial lymph node; rhesus macaque. The lymph node capsule is thickened, and there are foci of endometriosis in the capsule (arrow). HE.

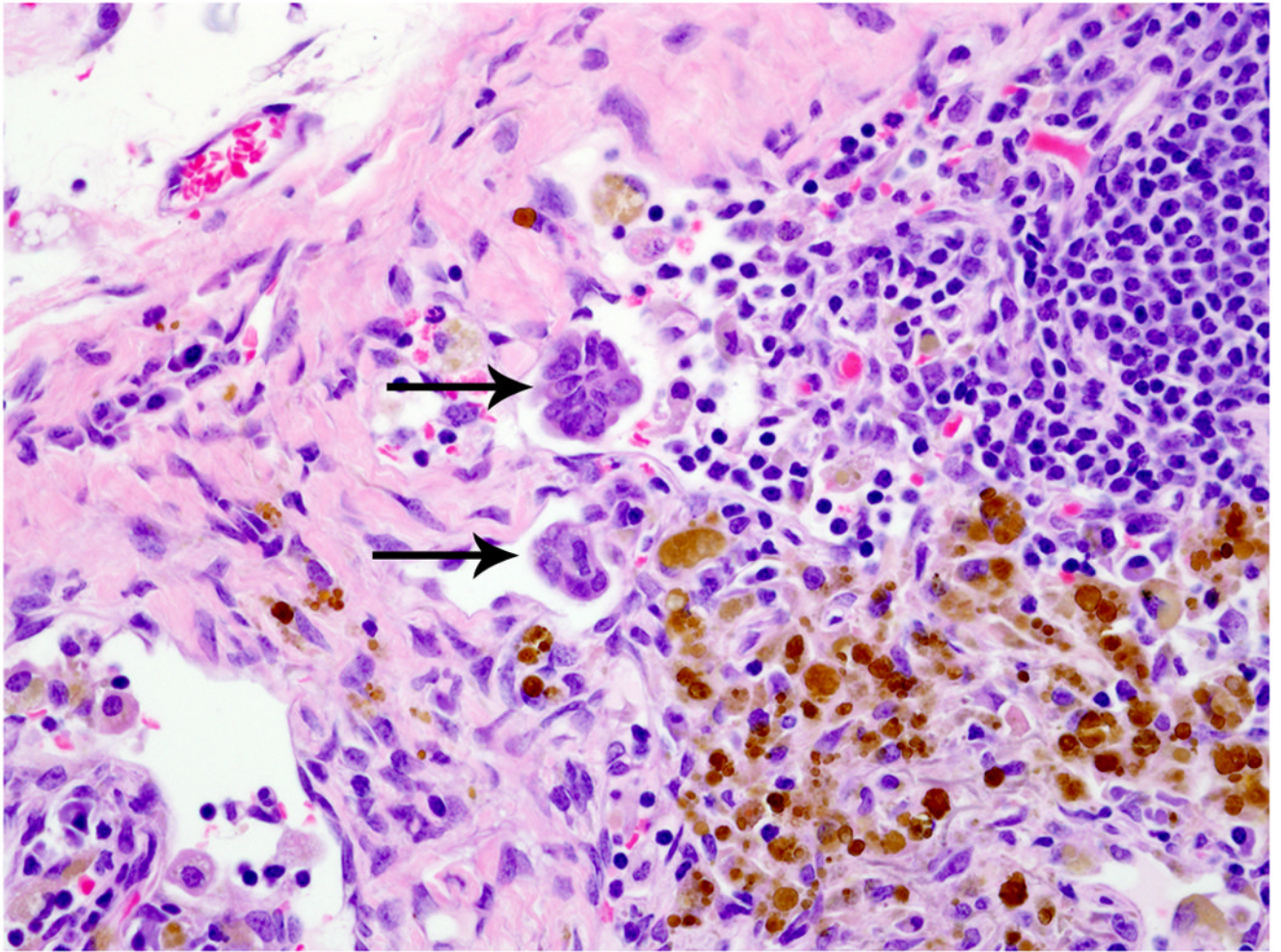


Figure 6. Tracheobronchial lymph node; rhesus macaque. Rafts of endometrial glands are present within the subcapsular sinuses of tracheobronchial lymph node (arrows). HE.

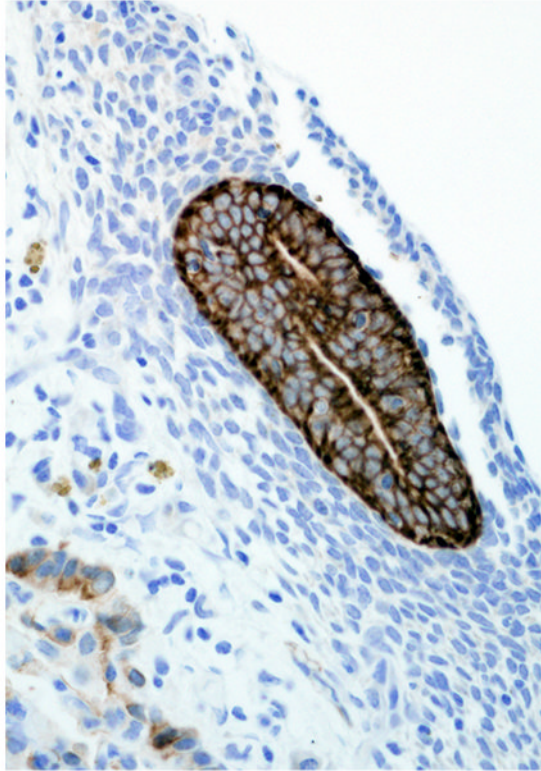


Figure 7. Pleural endometriosis, lung; rhesus macaque. Endometriotic glandular epithelium has strong immunoreactivity for cytokeratin. Immunoperoxidase staining, DAB chromogen, Mayer's hematoxylin counterstain.

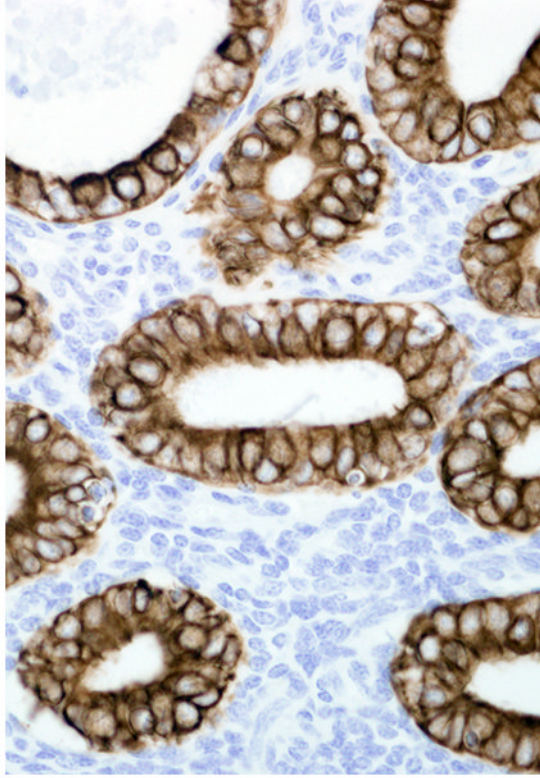


Figure 8. Endometrium; rhesus macaque. Glandular epithelial cells have strong immunoreactivity for cytokeratin. Immunoperoxidase staining, DAB chromogen, Mayer's hematoxylin counterstain.

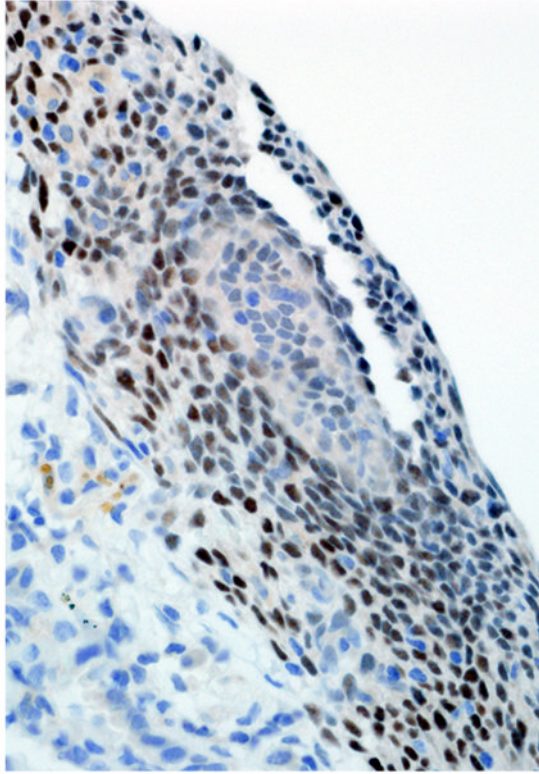


Figure 9. Pleural endometriosis, lung; rhesus macaque. There is strong intranuclear immunoreactivity in the endometriotic stroma and weak immunoreactivity in the epithelial cells for progesterone receptor. Immunoperoxidase staining, DAB chromogen, Mayer's hematoxylin counterstain.

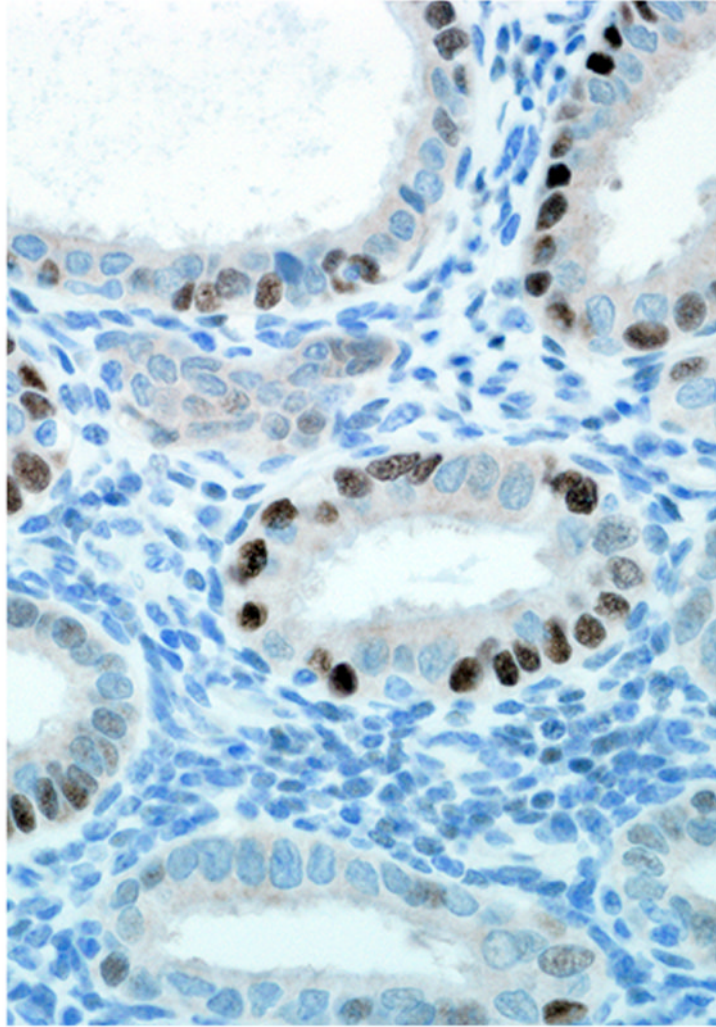


Figure 10. Endometrium; rhesus macaque. Roughly 50% of the glandular epithelial cells have strong nuclear immunoreactivity for progesterone receptor, and the stroma is negative. Immunoperoxidase staining, DAB chromogen, Mayer's hematoxylin counterstain.

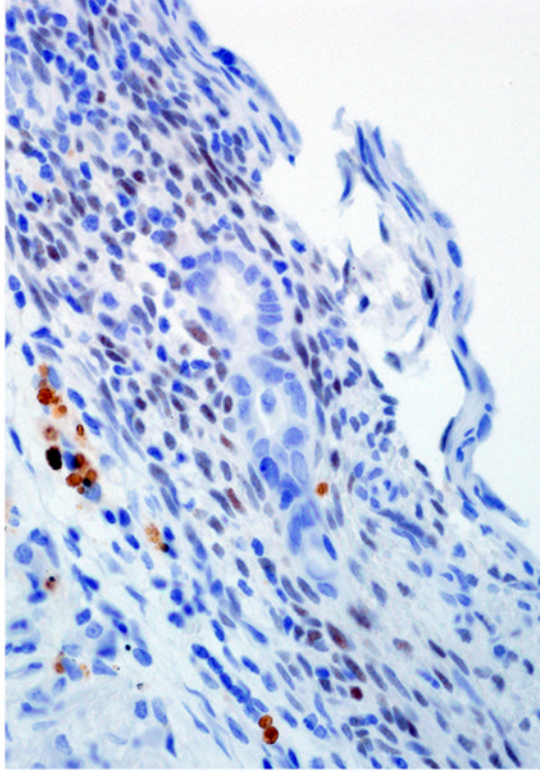


Figure 11. Pleural endometriosis, lung; rhesus macaque. There is scattered nuclear immunoreactivity for estrogen receptor in the stromal and epithelial cells of the endometriotic tissue. Immunoperoxidase staining, DAB chromogen, Mayer's hematoxylin counterstain.

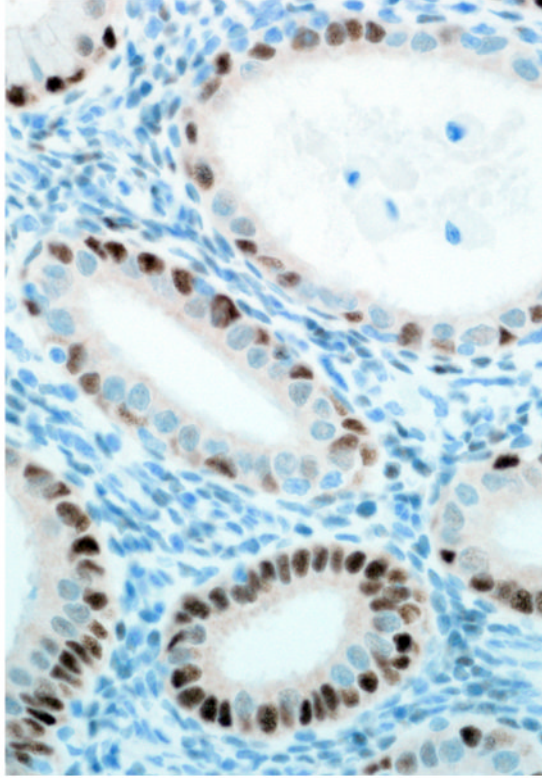


Figure 12. Endometrium; rhesus macaque. Roughly 75% of the glandular epithelial cells have strong nuclear immunoreactivity for estrogen receptor. Immunoperoxidase staining, DAB chromogen, Mayer's hematoxylin counterstain.

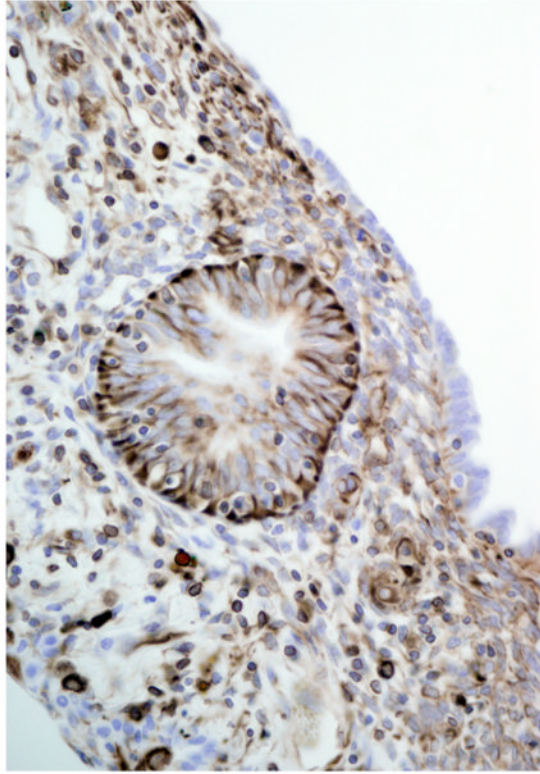


Figure 13. Pleural endometriosis, lung; rhesus macaque. Endometriotic tissue has strong cytoplasmic immunoreactivity for vimentin. Immunoperoxidase staining, DAB chromogen, Mayer's hematoxylin counterstain.

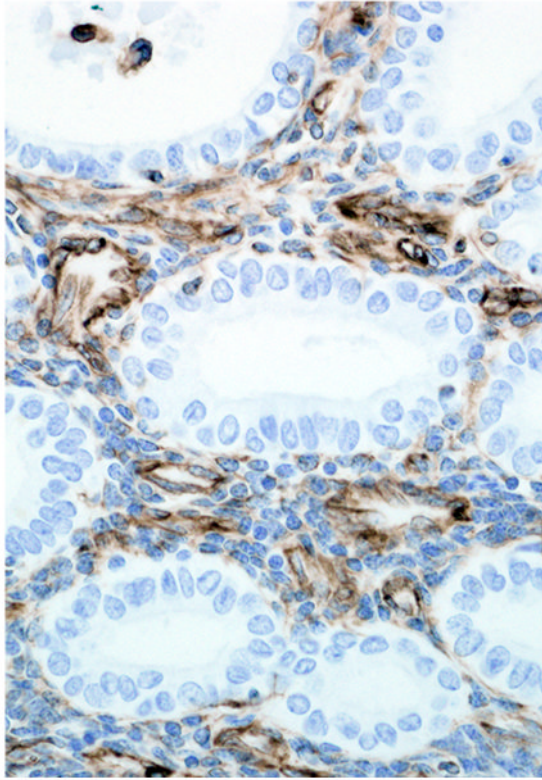


Figure 14. Endometrium; rhesus macaque. Stromal cells have strong intracytoplasmic immunoreactivity for vimentin. Immunoperoxidase staining, DAB chromogen, Mayer's hematoxylin counterstain.

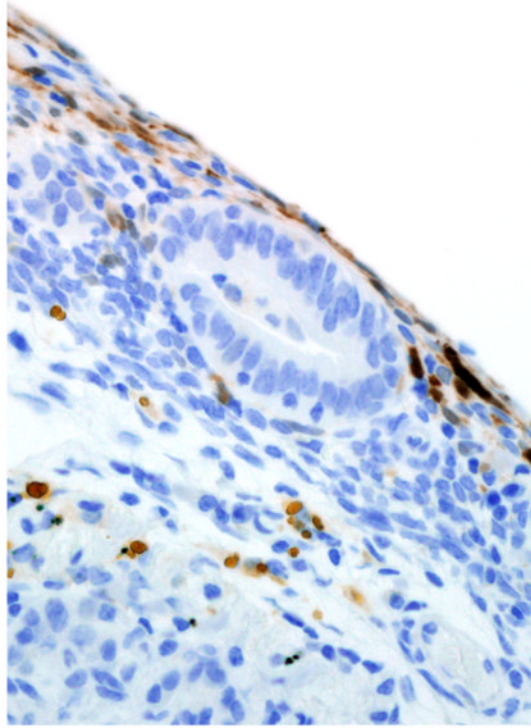


Figure 15. Pleural endometriosis, lung; rhesus macaque. Rare calretinin immunoreactive cells are present in the endometriotic stroma. Immunoperoxidase staining, DAB chromogen, Mayer's hematoxylin counterstain.

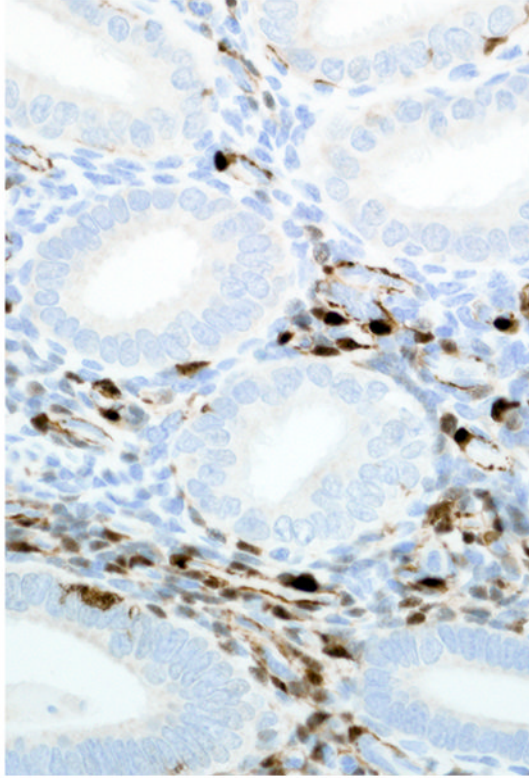


Figure 16. Endometrium; rhesus macaque. Roughly 50% of stromal cells have strong cytoplasmic immunoreactivity for calretinin. Immunoperoxidase staining, DAB chromogen, Mayer's hematoxylin counterstain.

Table 1
Pleural and Abdominal Endometriosis and Normal Endometrium: Immunohistochemistry Results

Marker	Pleural Endometriosis			Normal Endometriosis			Abdominal Endometriosis					
	Epithelium			Stroma			Epithelium			Stroma		
	INT ^a	DIS ^b	INT	DIS	INT	DIS	INT	DIS	INT	DIS	INT	DIS
Cytokeratin	+++	+++	-	-	+++	+++	-	-	+++	+++	+++	+
Vimentin	++	++	+++	+++	-	-	++	+++	++	++	++	+++
Progesterone Receptor	+	+++	+++	+++	+++	++	+	++	+++	+++	+++	+++
Estrogen Receptor	+	+	+	++	+++	+++	++	+++	+++	+++	+++	+++
Calretinin	-	-	++	+	-	-	+++	++	-	-	-	+
Carcinoembryonic antigen	-	-	-	-	-	-	-	-	-	-	-	-
Desmin	-	-	-	-	-	-	-	-	-	-	-	-

^aIntensity score: +++, strong; ++, moderate; +, weak; -, absent.

^bDistribution score: +++, 75%; ++, 25-75%; +, 25%; -, 0%.